Appraisal of the Kuo-Herling shell-model interaction and application to A=210–212 nuclei

E. K. Warburton
Brookhaven National Laboratory, Upton, New York 11973

B. A. Brown
Cyclotron Laboratory and Department of Physics and Astronomy, Michigan State University, East Lansing, Michigan 48824

(Received 11 September 1990)

Shell-model calculations are described for A=204–212 nuclei. These calculations use the Kuo-Herling realistic effective interactions for hole states and particle states relative to ^{208}Pb. These interactions contain a bare part and a core polarization contribution. The contribution of the core-polarization was varied to find the best fit to the energy spectra of A=204–206 and 210–212 nuclei. This and other modifications to the Kuo-Herling interaction—designed to give better agreement with experimental energy spectra—are discussed. Aspects of the spectroscopy of $^{211-212}$Pb, ^{210}Po, ^{212}Ra, ^{210}Bi, and ^{212}At are presented in order to illustrate the use of the Kuo-Herling particle interaction. Deficiencies in the Kuo-Herling interaction are described and the desirability and possibility of an improved calculation of the interaction is emphasized.

I. INTRODUCTION

The shell model has had enormous success in the lead region since the pioneering study of True and Ford who used a simple singlet-even neutron-neutron residual interaction to study ^{206}Pb.[1] Particularly successful has been the residual interaction of Kuo and Herling.[2] This interaction was derived by reaction matrix techniques developed by Kuo and Brown[3] from a free nucleon-nucleon potential[4] with renormalizations due to the truncated model space. It is therefore called an effective realistic interaction. The fact that effective realistic residual interactions give a good description of nuclei near closed shells throughout the periodic table is a great success for nuclear structure. Nevertheless, shell-model calculations—including the present ones—have revealed significant discrepancies in the Kuo-Herling interaction which can be laid to approximations made for reasons of computational simplicity, for instance, the use of harmonic-oscillator radial wave functions. However, no calculation of residual interactions via reaction matrix techniques using more realistic radial wave functions has ever appeared in the literature. In short, the Kuo-Herling interaction is the best realistic interaction available for $A \sim 208$ nuclei, and it is very worthwhile to examine its predictive powers in detail with a view to worthwhile modifications and future improvements.

In the $A < 208$ lead region, the lead isotopes have been a fruitful testing ground for the Kuo-Herling interaction. McGrory and Kuo[5] performed calculations for $^{204-206}$Pb and found a minor modification of the interaction resulted in improved agreement with experiment. More recently, Blomqvist *et al.*[6] obtained a very successful description of $^{204-206}$Pb by modifying selected two-body matrix elements (TBME) of the Kuo-Herling interaction. Such attention has not been given to the Pb isotopes above ^{208}Pb. One reason is that the shell-model calculations for $^{210-212}$Pb are technically more difficult. The Kuo-Herling model space is shown in Fig. 1. Note the hole space below ^{208}Pb is completely separate from the particle space above ^{208}Pb. There are six neutron orbits with a total m [$= \sum_j (2j+1)$] of 38 in the neutron hole space and seven orbits with m totaling 58 in the neutron particle space. The large number of active orbits and the presence of orbits with relatively high spin means untruncated calculations with more than two particles in the model space are quite demanding. In fact, there have been no published results of untruncated calculations for $^{211-212}$Pb performed with the Kuo-Herling interaction. The difficulty of handling these large scale calculations was discussed by McGrory and Kuo[5] who did study these nuclei in a truncated basis. One motive for the present study was to test the Kuo-Herling neutron-particle interaction as fully as the rather meager experimental data[7,8,9] will allow. However, the major motive was more general, namely, to assess the Kuo-Herling particle (KHP) interaction for both neutrons and protons as fully as has been done for the Kuo-Herling hole (KHH) interaction, to see if (and what) minor modifications to the KHP interaction will give significantly improved agreement with experimental binding energies, both absolute and relative, and to gain information of value in future calculations of effective realistic interactions in the lead region.

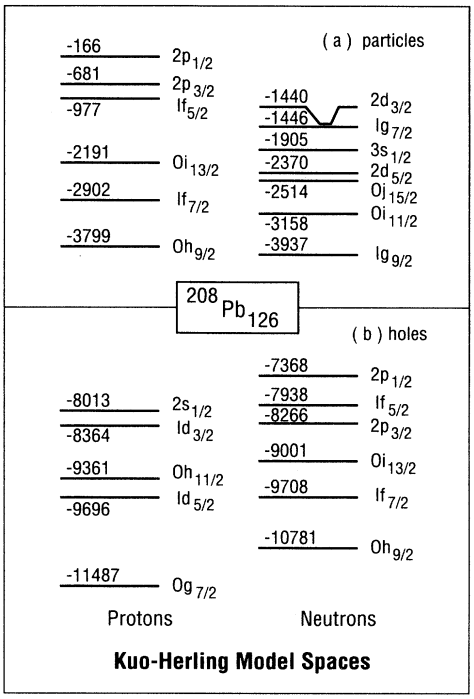

FIG. 1. The Kuo-Herling model spaces for the lead region. Single-particle energies (in keV) are taken from the experimental spectra of A=207 and 209 nuclei and are relative to ^{208}Pb.

II. ORIENTATION

For each TBME the Kuo-Herling interaction has a bare matrix element, a 1p-1h core polarization "bubble" and a further renormalization due to 2p-2h excitations. We designate the three constituents of the interaction in an obvious notation as $G_{\rm bare}$, $G_{\rm 1p1h}$, and $G_{\rm 2p2h}$. We will refer to the neutron-neutron, proton-neutron, and proton-proton parts of the interactions as nn, pn, and pp. The construction and use of the Kuo-Herling interactions is described by McGrory and Kuo[5] in more detail than in Ref. 2. One might ask if current nucleon-nucleon potentials give significantly different results than those derived by the Kuo-Brown method from the 1962 Hamada-Johnston potential. We address this question by comparing, in Table I, calculations for 22 nn TBME applicable to the KHH (hole) space of Fig. 1. The bare TBME labeled H7B are the results of a potential due to Hosaka, Kubo, and Toki.[10] The H7B potential is expressed as a superposition of seven one-boson-exchange potentials, the oscillator matrix elements of which were fit to the G-matrix elements derived from the Paris[11] nucleon-nucleon potential. The earlier M3Y interaction[12,13] is based on the Hamada-Johnston[4] and Reid[14] potentials. It is discussed by Hosaka, Kubo, and Toki. We evaluate both the M3Y and H7B TBME using harmonic-oscillator (HO) wave functions with an $\hbar\omega$ of 7 MeV which was the value used by Kuo and Herling. The three calculations of $G_{\rm bare}$ are in relatively good agreement. The H7B potential gives TBME which average 16% stronger than the TBME of KHP $G_{\rm bare}$, and, if this scaling is made, the agreement is very good. We note that the H7B potential was derived for lighter nuclei (A=16, 40, 90) and the scaling to be used in extrapolation to the lead region is somewhat uncertain.[10]

McGrory and Kuo[5] showed that the interaction $G_{\rm bare}+G_{\rm 1p1h}$ represented the experimental energy spectra of ^{206}Pb better than $G_{\rm bare}+G_{\rm 1p1h}+G_{\rm 2p2h}$. This is also the case for Kuo-Brown interactions in other regions of A. Based on mathematical analogy to a study of multiparticle forces in truncated shell-model spaces, Gambhir[15] has speculated that the contribution of $G_{\rm 3p3h}$ would largely cancel that of $G_{\rm 2p2h}$. This is only one possible reason why it is found empirically that $G_{\rm 2p2h}$ is best neglected. McGrory and Kuo also found better agreement for ^{206}Pb if $G_{\rm 1p1h}$ was weakened somewhat. This finding was the stimulus for our approach, which is to vary the constants $K_{\rm bare}$ and $K_{\rm ph}$ in $G = K_{\rm bare}G_{\rm bare} + K_{\rm ph}G_{\rm 1p1h}$ so as to obtain best agreement with experimental binding energies and level schemes. Possible defects in the Kuo-Herling interaction were considered briefly by Bergstrom, Blomqvist, Herrlander, and Linden.[16] One defect in both $G_{\rm bare}$ and $G_{\rm 1p1h}$ is that they were calculated with HO wave functions, and it is known that these can give a rather poor representation of the radial wave functions of orbitals in the heavier nuclei. Bergstrom *et al.*[16] presented arguments indicating that the error in $G_{\rm bare}$ associated with the use of HO wave functions could be ~30%. They also pointed out that $G_{\rm 1p1h}$ was calculated with a constant $2\hbar\omega$ = 14 MeV for the energy separation of the particle and hole and that the effective energy denominator in the calculation should probably average more than this and, of course, vary with the specific orbits. We shall return to the question of Woods-Saxon (WS) vs HO wave functions in Sec. V. For the present we note that there are several sources of such inaccuracies which might lead to an average $G = G_{\rm bare} + G_{\rm 1p1h}$ which differs by ~10–30 % from the Kuo-Herling values. This preamble, then, is intended as a justification for our purely pragmatic approach of the scaling of the interaction.

An orientation towards the relative importance of the ingredients of the Kuo-Herling interaction can be had by considering Table II, which lists several possible averages for the TBME. The two pp interactions are not listed in this table because they include the two-body Coulomb contribution which averages ~250 keV for diagonal TBME and ~ 0 keV for off-diagonal TBME. This Coulomb contribution masks the relative values of the nuclear part of the interaction which is quite similar for pp and nn. Averages for $\langle j_1 j_2|V|j_3 j_4\rangle_J$ are given for J=0 and J >0 separately to better illustrate their different behavior. Thus we note the following features deduced from average values of $|\langle j_1 j_2|V|j_3 j_4\rangle_J|$, denoted $\langle$abs(G)$\rangle$:

(1a) $G_{\rm 1p1h}$ is quite important;

(2a) $G_{\rm 2p2h}$ is important for J=0, unimportant for

TABLE I. Selected neutron-neutron two-body matrix-elements illustrating the degree of agreement between the M3Y interaction of Bertsch *et al.* (Ref. 12), the H7B interaction of Hosaka, Kubo, and Toki (Ref. 10) and the Kuo and Herling interaction (Ref. 2) for the bare G-matrix TBME (labeled $G_{\rm bare}$). The 1p-1h renormalization of the Kuo-Herling TBME (labeled $G_{\rm 1p1h}$) is also included to illustrate the magnitude of the renormalization due to the finite model space.

j_1	j_2	J^π	$\langle j_1 j_2 \vert V \vert j_1 j_2 \rangle_J$			
			$G_{\rm bare}$ (M3Y)	$G_{\rm bare}$ (H7B)	$G_{\rm bare}$ (KUO)	$G_{\rm 1p1h}$ (KUO)
$h_{9/2}$	$h_{9/2}$	0^+	−0.1346	−0.2280	−0.1906	−0.6859
	$h_{9/2}$	2^+	−0.2283	−0.2780	−0.2474	−0.0860
	$h_{9/2}$	4^+	−0.0971	−0.1279	−0.1119	+0.1104
	$h_{9/2}$	6^+	−0.0396	−0.0634	−0.0501	+0.1772
	$h_{9/2}$	8^+	+0.0085	−0.0088	+0.0003	+0.1846
$h_{9/2}$	$i_{13/2}$	2^+	−0.0820	−0.2082	−0.1636	−0.1961
	$i_{13/2}$	3^+	+0.0054	−0.0609	−0.0562	−0.0990
	$i_{13/2}$	4^+	−0.0495	−0.0912	−0.0691	+0.0493
	$i_{13/2}$	5^+	−0.0211	−0.0529	−0.0423	+0.0509
	$i_{13/2}$	6^+	−0.0567	−0.0864	−0.0721	+0.1152
	$i_{13/2}$	7^+	−0.0814	−0.0995	−0.0853	+0.1152
	$i_{13/2}$	8^+	−0.0598	−0.0860	−0.0738	+0.1384
	$i_{13/2}$	9^+	−0.1970	−0.2054	−0.1736	+0.1469
	$i_{13/2}$	10^+	−0.0659	−0.0904	−0.0814	+0.1627
	$i_{13/2}$	11^+	−0.6525	−0.6559	−0.5486	+0.1383
$i_{13/2}$	$i_{13/2}$	0^+	−0.2127	−0.2996	−0.2926	−0.7232
	$i_{13/2}$	2^+	−0.3296	−0.3830	−0.3495	−0.2090
	$i_{13/2}$	4^+	−0.1610	−0.1941	−0.1732	−0.0319
	$i_{13/2}$	6^+	−0.0967	−0.1219	−0.1041	+0.0445
	$i_{13/2}$	8^+	−0.0614	−0.0831	−0.0687	+0.0817
	$i_{13/2}$	10^+	−0.0339	−0.0538	−0.0412	+0.1052
	$i_{13/2}$	12^+	−0.0012	−0.0177	−0.0067	+0.1250

TABLE II. Various averages for the Kuo-Herling TBME.

Space	Average	Range	$G_{\rm Bare}$	$G_{\rm 1p1h}$	$G_{\rm 2p2h}$	No.
			Holes			
nn	$\langle G \rangle$	$J^\pi \neq 0^+$	−0.032	+0.013	−0.001	332
nn	$\langle \mathrm{abs}(G) \rangle$	$J^\pi \neq 0^+$	+0.065	+0.054	+0.003	332
nn	$\langle G \rangle$	$J^\pi = 0^+$	−0.115	−0.115	−0.042	21
nn	$\langle \mathrm{abs}(G) \rangle$	$J^\pi = 0^+$	+0.331	+0.234	+0.067	21
pn	$\langle G \rangle$	$J^\pi \neq 0^+$	−0.062	+0.009	−0.002	784
pn	$\langle \mathrm{abs}(G) \rangle$	$J^\pi \neq 0^+$	+0.120	+0.052	+0.004	784
pn	$\langle G \rangle$	$J^\pi = 0^+$	−0.205	+0.082	−0.000	10
pn	$\langle \mathrm{abs}(G) \rangle$	$J^\pi = 0^+$	+0.491	+0.131	+0.001	10
			Particles			
nn	$\langle G \rangle$	$J^\pi \neq 0^+$	−0.021	+0.000	−0.001	683
nn	$\langle \mathrm{abs}(G) \rangle$	$J^\pi \neq 0^+$	+0.047	+0.030	+0.001	683
nn	$\langle G \rangle$	$J^\pi = 0^+$	−0.112	−0.078	−0.027	28
nn	$\langle \mathrm{abs}(G) \rangle$	$J^\pi = 0^+$	+0.272	+0.113	+0.042	28
pn	$\langle G \rangle$	$J^\pi \neq 0^+$	−0.041	+0.003	−0.001	1746
pn	$\langle \mathrm{abs}(G) \rangle$	$J^\pi \neq 0^+$	+0.082	+0.033	+0.004	1746
pn	$\langle G \rangle$	$J^\pi = 0^+$	−0.121	+0.018	−0.006	16
pn	$\langle \mathrm{abs}(G) \rangle$	$J^\pi = 0^+$	+0.369	+0.053	+0.025	16

$J>0$.

And from the average values of $\langle j_1 j_2|V|j_3 j_4\rangle_J$, denoted $\langle G\rangle$:

(1b) $\langle G_{\rm bare}\rangle$ and $\langle G_{\rm 2p2h}\rangle$ are always attractive;

(2b) $\langle G_{\rm 1p1h}\rangle$ is attractive for $J=0$;

(3b) $\langle G_{\rm 1p1h}\rangle$ is repulsive for $J>0$.

A general defect of the Kuo-Herling interaction, $G_{\rm bare} + G_{\rm 1p1h}$, is that it overbinds 0^+ ground states relative to absolute binding energies and to $J>0$ states. This defect may be due to the difficulty of calculating the pairing energy which appears to have a strong density dependence.[17] The overbinding of the 0^+ ground states is obviously increased when $G_{\rm 2p2h}$ is included as follows from (2a) and (1b). We have also found that the effect of $G_{\rm 2p2h}$ can be simulated by increasing $G_{\rm 1p1h}$ somewhat. Thus, we drop $G_{\rm 2p2h}$ from further consideration.

In the lowest order we find, with the exception of 0^+ states, that what is needed to increase the agreement with experimental level schemes is to decrease the importance of $G_{\rm 1p1h}$ in $G = K_{\rm bare}G_{\rm bare} + K_{\rm ph}G_{\rm 1p1h}$. This can be done by increasing $K_{\rm bare}$ or decreasing $K_{\rm ph}$, or both. However, for $J^\pi = 0^+$ states, which are generally too bound, increasing $K_{\rm bare}$ makes the problem worse because of the very attractive values of $G_{\rm bare}$ for $J=0$ apparent in Tables I and II. Thus we shall restrict our discussion to varying $K_{\rm ph}$ with $K_{\rm bare}=1$ although the variance of both was studied.

III. CALCULATIONS

In our approach the TBME are given by

$$\langle j_1 j_2|V|j_3 j_4\rangle = \langle j_1 j_2|V|j_3 j_4\rangle_{\rm bare} + K_{\rm ph}\langle j_1 j_2|V|j_3 j_4\rangle_{\rm 1p\text{-}1h} \ . \tag{1}$$

Our shell-model calculations, performed with the computer code OXBASH,[18] reproduced the results of Kuo and Herling[2] and of McGrory and Kuo[5] when using their values of $K_{\rm ph}$ and single-particle energies. The results given here, however, use the single-particle energies (SPE) of Fig. 1. These are based on the yrast levels of the appropriate spin and parity as reported in the Nuclear Data Sheets for $A=207$ (Ref. 19) and $A=209$.[20] The changes are mainly due to small changes in binding energies since 1971. However, a new $\frac{1}{2}^-$ level at 3633 keV in ^{209}Bi is identified with the $\pi 2p_{1/2}$ orbital.[20] We emphasize that we, as well as other users of the Kuo-Herling interaction, determine the SPE from yrast states in the $A=207$ and 209 nuclei. Any difference between the yrast state and the centroid energy of a specific orbital—as determined by one-nucleon transfer reactions—presumably reflects the influence of particle-hole excitations which may have nontrivial consequences and are thus a further source of possible disagreement with experiment. A specific example is the octupole coupling of core-excited states as discussed, for example, by Poletti *et al.*[21]

Harmonic-oscillator (HO) radial wave functions were used in calculations of the TBME, while Woods-Saxon (WS) forms were used in the calculations of some one-body observables. For the Woods-Saxon radial wave functions the parameters of Streets, Brown, and Hodgson[22] were used. These reproduce the experimental rms charge radius of ^{208}Pb of 5.503(2) fm and give a neutron rms radius 0.2 fm larger. With normal shell occupancies, these radii correspond to $\hbar\omega = 6.701$ and 7.183 MeV for protons and neutrons, respectively. For HO wave functions we use the average $\hbar\omega$ of 6.942 MeV for integrals involving both neutron and proton wave functions. Kuo and Herling used $\hbar\omega = 7.0$ MeV in their calculations of TBME in close agreement with this "best" effective value.

The determination of the $K_{\rm ph}$ of Eq. (1) was made by comparison to experimental level energies of low-lying levels. Three parameters are relevant to this determination. If we define

$$\Delta E_B^{(i)} = E_B({\rm expt})_i - E_B({\rm KH}x)_i \ , \tag{2}$$

where E_B is a binding energy (taken here as relative to that of ^{208}Pb), i extends over n known low-lying experimental (expt) levels and KHx stands for KHH (Kuo-Herling hole) or KHP (Kuo-Herling particle). Then the three quantities are defined as follows:

$$\langle \Delta E_B\rangle = \frac{1}{n}\sum_{i=1}^{n}\Delta E_B^{(i)} \ , \tag{3}$$

$$\langle \Delta E_B\rangle_{\rm rms} = \frac{1}{n}\left(\sum_{i=1}^{n}(\Delta E_B^{(i)})^2\right)^{\frac{1}{2}} \ , \tag{4}$$

and

$$\langle \Delta E_x\rangle_{\rm rms} = [{\rm abs}(\langle \Delta E_B\rangle_{\rm rms}^2 - \langle \Delta E_B\rangle^2)]^{\frac{1}{2}} \ . \tag{5}$$

All three quantities were followed as $K_{\rm ph}$ was varied. The aim was to find a value of $K_{\rm ph}$ for which the interaction gave the best agreement with the experimental level spectrum. In general, it was found that $\langle \Delta E_x\rangle_{\rm rms}$ had a shallow minimum so that the best value of $K_{\rm ph}$ was uncertain by $\pm$ ~0.05 and that over a range of $\pm$ ~0.3 about this value $\langle \Delta E_B\rangle$ was essentially constant. This latter point can be inferred from the fact that $\langle G_{\rm 1p1h}\rangle$ for all J is quite small as can be seen by combining the $J=0$ and $J>0$ results of Table II. We first consider the KHH results for $\langle \Delta E_x\rangle_{\rm rms}$ and $\langle \Delta E_B\rangle$ which are summarized in Table III.

For the *nn* hole interaction the three and four particle systems were considered as well as the two particle systems. For these the quality of the fit is noticeably more sensitive to $K_{\rm ph}$ so that these nuclei had more weight in the fixing of $K_{\rm ph}$ than the two neutron system. We see that the "best fit" for the *nn* interaction as determined by $\langle E_x\rangle_{\rm rms}$ occurs at the small value for $K_{\rm ph}$ of 0.55 (McGrory and Kuo[5] used 0.75). Such a small value results

TABLE III. $\langle\Delta E_x\rangle_{\rm rms}$ and $\langle\Delta E_B\rangle$ values (in keV) for A=204–206 nuclei. $\langle\Delta E_B\rangle$ is the amount by which the nucleus is overbound (relative to ^{208}Pb) and $\langle\Delta E_x\rangle_{\rm rms}$ is the mean-square deviation of the excitation energies, both quantities being determined by comparison to n experimental energy levels.

		$K_{\rm ph}$ varied		$K_{\rm ph}$=1		
Nucleus	$K_{\rm ph}$	$\langle\Delta E_x\rangle_{\rm rms}$	$\langle\Delta E_B\rangle$	$\langle\Delta E_x\rangle_{\rm rms}$	$\langle\Delta E_B\rangle$	n
^{206}Hg	0.70	42	59	69	120	3
^{206}Tl	0.75	83	24	96	3	18
^{206}Pb	0.55	59	77	86	90	21
^{205}Pb	0.55	94	228	167	271	18
^{204}Pb	0.55	95	471	162	677	23

because of the overbinding of the 0^+ ground states of ^{204}Pb and ^{206}Pb. The small value of $K_{\rm ph}$ is disturbing because it changes the wave functions of the 0^+ ground states significantly away from the $K_{\rm ph} \geq 0.75$ values and from experiment.[23,24] Blomqvist and collaborators[6,25] have adopted an approach better tuned to the major deficiency in the KHH interaction. They modify individual TBME so as to better reproduce energy spectra, spectroscopic factors, and electromagnetic properties. An examination of their results for ^{204}Pb, ^{206}Pb, and ^{206}Hg reveals that the most important change was to decrease the binding of the 0^+ diagonal TBME relative to the other diagonal TBME which have observable influence on the low-lying spectra. We consider this approach more relevant for the KHH interaction and recommend the use of their TBME or of others similarly derived.

The results for the KHP interaction are quite different. As seen in Table IV the "best-fit" value of $K_{\rm ph}$ is close to unity—well within the range of uncertainty which seems reasonable. Nevertheless, the changes in the energy spectra from those for $K_{\rm ph}$ = 1 are significant. We illustrate this by Table V where the ^{212}Rn levels used in the fits of Eqs. (3)–(5) are compared to the predictions for $K_{\rm ph}$=0.92 and 1.0. It is clear that $K_{\rm ph}$=0.92 reproduces the low-lying spectrum (E_x <3.5 MeV) significantly better than $K_{\rm ph}$ = 1.0. The poor agreement for E_x >3.5 MeV will be discussed in Sec. IV A.

Further binding energies used to appraise the success of the interactions are summarized in Table VI. Note that these are ground-state binding energies, not the average binding energies of Table IV. The shell-model calculations for the A=212 isotopes of Bi, Po, and At have quite large dimensions and are at the limit of our computational resources. Thus not all levels of these three nuclei could be handled. In Tables IV and VI the quantity $\Delta^{(\alpha)}$ ($\alpha \equiv pp, nn, pn$) is a constant energy added to all the diagonal TBME of a particular type α. The purpose is to improve the predictive power for absolute binding energies. As shown by a comparison of columns A and B in Tables IV and VI, the improvement is considerable, especially for the A=212 nuclei. The $\Delta^{(\alpha)}$ were determined by a least-squares fit to the data in the tables. The results are $\Delta(pp)$=+49 keV, $\Delta(pn)$ = −53 keV, and $\Delta(nn)$=+15 keV. Note that these changes do not affect wave functions or energy spectra, only absolute binding energies. The interaction with $\Delta^{(\alpha)} \neq 0$ is the starting point for the interaction labeled KHP$_e$ which will be discussed in Sec. IV C.

TABLE IV. $\langle\Delta E_x\rangle_{\rm rms}$ and $\langle\Delta E_B\rangle$ values (in keV) for A=210–212 nuclei. $\langle\Delta E_B\rangle$ is the amount by which the nucleus is overbound (relative to ^{208}Pb) and $\langle\Delta E_x\rangle_{\rm rms}$ is the mean-square deviation of the excitation energies, both quantities being determined by comparison to n experimental energy levels.

		$K_{\rm ph}$ varied			$K_{\rm ph}$=1		
Nucleus	$K_{\rm ph}$	$\langle\Delta E_x\rangle_{\rm rms}$	$\langle\Delta E_B\rangle$		$\langle\Delta E_x\rangle_{\rm rms}$	$\langle\Delta E_B\rangle$	n
			A[a]	B[b]		A[a]	
^{210}Pb	1.07	23	−15	−30	30	−23	6
^{211}Pb	1.07	36	51	−39	44	53	5
^{212}Pb	1.07	36	51	−39	44	53	5
^{210}Bi	0.90	71	−55	−2	76	−54	28
^{210}Po	0.92	67	49	0	64	55	24
^{212}Rn	0.92	68	282	− 12	94	310	12

[a] $\Delta^{(\alpha)}$=0.
[b] $\Delta^{(\alpha)}$ as given in text.

TABLE V. Comparison of the energy spectrum of ^{212}Rn to the KHP predictions for K_{ph} = 0.92 and 1.00. The first twelve energy levels listed were used to determine the "best-fit" value of K_{ph} via Eq. (3). Those marked with an asterisk were not included in this fit. The index k orders states of a given J^π in energy. ΔE_x is experiment–model and is positive if the model prediction is too bound.

Expt			$K_{ph}=0.92$		$K_{ph}=1.00$	
E_x (keV)	J^π	k	E_x (keV)	ΔE_x (keV)	E_x (keV)	ΔE_x (keV)
0	0^+	1	0	0	0	0
1274	2^+	1	1333	− 59	1409	− 135
1501	4^+	1	1560	− 59	1662	− 161
1640	6^+	1	1646	− 6	1744	− 105
1694	8^+	1	1667	+ 27	1768	− 97
2116	8^+	2	2110	+ 6	2200	− 84
2304	4^+	2	2287	+ 17	2304	− 122
2761	11^-	1	2585	+ 176	2737	+ 44
2655	10^+	1	2732	− 77	2632	− 271
2881	12^+	1	2959	− 78	2859	− 286
3358	14^+	1	3287	+ 71	3335	− 126
3298	12^+	2	3305	− 7	3275	− 199
4067	17^-	1	*3761	+ 306	*3963	+ 104
3991	15^-	1	*3767	+ 224	*3961	+ 30
4135	16^-	1	*3834	+ 301	*4034	+ 101
4583	17^-	2	*4373	+ 210	*4555	+ 28
5115	18^-	1	*4416	+ 699	*4609	+ 506
5427	20^+	1	*4918	+ 509	*5125	+ 302
6167	20^+	2	*6125	+ 42	*6326	− 159
5772	19^-	1	*6773	−1007	*6973	−1201

IV. SOME CONSIDERATION OF THE SPECTROSCOPY

A. ^{211}Pb and ^{212}Pb

The predicted spectrum of ^{211}Pb is listed in Table VII and comparison to the experimentally known level spectrum is made in Fig. 2. The experimental information is from the ^{210}Pb$(t,d)^{211}$Pb study of Ellegaard, Barnes, and Flynn[26] with the exception of the two probable levels at 439 and 445 keV which are from ^{215}Po α decay.[8] The KHP predictions give a quite satisfactory account of the observed stripping strength. First note that for each of the seven orbitals the centroid of the strength is in close agreement with experiment. Of the 52 predicted energy levels for $E_x < 2.7$ MeV (see Table VII) only thirteen have predicted S values large enough to be observed. Only these thirteen and four more are included in Fig. 2. Considering the predictions to the left of the figure, several features are of interest. The stripping strength for the $1g_{9/2}$ and $0j_{15/2}$ orbitals is mainly in the yrast state as expected although there is a discrepancy in the absolute values of S. For $0i_{11/2}$, some observable strength is predicted in the k=3 level as well as k=1. An experimental candidate for the $\frac{11}{2}^+_3$ level at 1377 keV is indicated. The $1g_{7/2}$ strength is predicted to be shared by the k=7,8,10 levels, and this is consistent with experiment. The $2d_{5/2}$ strength is predicted to be concentrated in the k=2 state, again this is consistent with experiment. Note that the nonobservation of the $k < 7$, $\frac{7}{2}^+$ and k= 1, $\frac{5}{2}^+$ states is a success for the predictions. Now consider the predictions for the $3s_{1/2}$ and $2d_{3/2}$ orbitals shown on the right. For these the detailed splitting of the strength is not in very good agreement with experiment. The observed strength is fragmented more than is predicted. This fragmentation is also indicated by the observation of more levels than are predicted to be observable. Finally, we note that the sharing of strength for the $1g_{7/2}$, $3s_{1/2}$, and $2d_{3/2}$ orbitals is quite sensitive to the wave functions; for instance, it varied considerably as K_{ph} was varied.

The spectrum of ^{212}Pb is listed in Table VIII. Quite

TABLE VI. Ground-state binding energies for A=210 and 212 nuclei.

Nucleus	Binding energy		ΔE_B (g.s.)	
	Expt	Model[a]	A[a]	B[b]
^{210}Pb	--9 122	−9 106	− 16	− 31
^{210}Bi	−8 403	−8 380	− 23	− 30
^{210}Po	−8 782	−8 811	+ 29	− 20
^{212}Pb	−18 084	−18 124	+ 40	− 50
^{212}Bi	−17 873	−17 850	− 23	− 86
^{212}Po	−19 342	−19 063	−276	−131
^{212}At[c]	−16 581	−16 600	+ 19	+ 31
^{212}Rn	−16 066	−16 359	+293	− 1

[a] $\Delta^{(\alpha)}$=0.
[b] $\Delta^{(\alpha)}$ as given in text.
[c] The J^π=9$^-$ state at 225 keV.

complete listings of this and the ^{211}Pb and ^{212}Rn KH spectra are presented because they have not been published previously, are difficult to obtain, and, we believe, should be generally available. Experimentally, only the 0^+–8^+ ground-state "band" and a probable 3^- level at 1.82 MeV have been identified in ^{212}Pb.[9] We were unable to diagonalize all the odd-parity spectrum; however, the 3_1^- level is predicted at 2.18 MeV. A sorting of selected states of ^{212}Pb by the dominant configuration is shown in Fig. 3. There is not much mixing between states with the exception of the 0^+–8^+ $g_{9/2}^4$ levels. An interesting prediction is that the predominantly $g_{9/2}^4$ 10^+ state is not yrast. The difference between the wave functions of the lowest two $J^\pi=10^+$ and 12^+ states is exemplified by the quadrupole and dipole moments shown in Fig. 3.

It was found by McGrory and Kuo[5] that the 0^+–8^+ ground-state "band" was dominated by $g_{9/2}^4$ with one $g_{9/2}$ pair coupled to zero. The wave-function composition we find for this band is shown in Table IX. It is seen to have considerable collectivity in the sense that, unlike the general trend of rather pure single-particle states, there are significant contributions from multiple configurations and the contributions are similar for the five states. Also shown in this table are the quadrupole moments and $B(E2)$ values for this band. These were calculated with the Woods-Saxon parameters of Streets *et al.*[22] and an effective neutron charge of $1.0e$.

B. ^{210}Po and ^{212}Rn

Historically ^{210}Po has provided valuable information on the effective two-nucleon interaction. Schiffer and

TABLE VII. KHP predictions for the energy spectrum of ^{211}Pb for $K_{\rm ph}=1.07$. The index k orders states of a given J^π in energy. Levels with $k\leq 10$ are shown for $E_x<2.7$ MeV while only k=1–2 levels are shown for $E_x>2.7$ MeV.

E_x (keV)	J^π	k	E_x (keV)	J^π	k	E_x (keV)	J^π	k	E_x (keV)	J^π	k
0	$9/2^+$	1	1890	$13/2^+$	4	2319	$15/2^+$	6	2574	$29/2^+$	1
499	$7/2^+$	1	1909	$1/2^+$	2	2320	$5/2^-$	2	2577	$21/2^-$	1
682	$5/2^+$	1	1910	$5/2^+$	5	2344	$13/2^+$	7	2583	$21/2^+$	4
693	$11/2^+$	1	1923	$11/2^+$	6	2352	$9/2^-$	2	2601	$1/2^+$	4
774	$13/2^+$	1	1924	$15/2^+$	4	2354	$1/2^-$	1	2615	$27/2^-$	1
826	$3/2^+$	1	1950	$9/2^+$	7	2355	$1/2^+$	3	2618	$25/2^+$	2
829	$11/2^+$	2	1960	$19/2^+$	2	2360	$7/2^+$	9	2629	$21/2^-$	2
923	$9/2^+$	2	1960	$7/2^+$	5	2365	$13/2^-$	2	2633	$9/2^-$	3
1043	$17/2^+$	1	1967	$11/2^+$	7	2369	$15/2^-$	3	2643	$15/2^-$	5
1057	$15/2^+$	1	1981	$5/2^+$	6	2378	$5/2^-$	3	2646	$23/2^+$	3
1151	$21/2^+$	1	1983	$9/2^+$	8	2437	$11/2^+$	9	2652	$9/2^-$	4
1353	$11/2^+$	3	2004	$17/2^+$	3	2442	$13/2^-$	3	2652	$17/2^+$	7
1376	$15/2^-$	1	2011	$13/2^+$	5	2444	$7/2^+$	10	2656	$3/2^+$	7
1386	$13/2^+$	2	2013	$13/2^-$	1	2458	$7/2^-$	2	2677	$23/2^-$	2
1414	$5/2^+$	2	2031	$19/2^+$	3	2462	$17/2^+$	5	2702	$25/2^-$	1
1458	$9/2^+$	3	2036	$7/2^+$	6	2465	$17/2^-$	2	2766	$27/2^+$	2
1472	$15/2^+$	2	2036	$17/2^+$	4	2469	$5/2^+$	8	2770	$27/2^-$	2
1531	$7/2^+$	2	2045	$15/2^+$	5	2484	$7/2^-$	3	2831	$25/2^-$	2
1553	$9/2^+$	4	2046	$21/2^+$	3	2492	$17/2^-$	3	2832	$31/2^-$	1
1658	$9/2^+$	5	2065	$23/2^+$	2	2510	$3/2^+$	6	2888	$29/2^-$	1
1672	$7/2^+$	3	2108	$15/2^-$	2	2511	$13/2^+$	8	2938	$33/2^-$	1
1682	$17/2^+$	2	2139	$3/2^+$	4	2511	$11/2^+$	10	2958	$35/2^-$	1
1690	$11/2^+$	4	2145	$11/2^-$	1	2512	$7/2^-$	4	2996	$29/2^-$	2
1693	$19/2^+$	1	2156	$13/2^+$	6	2520	$3/2^-$	2	3078	$1/2^-$	2
1706	$27/2^+$	1	2193	$7/2^-$	1	2530	$19/2^+$	4	3105	$31/2^-$	2
1732	$5/2^+$	3	2196	$9/2^-$	1	2530	$11/2^-$	3	3458	$33/2^-$	2
1744	$23/2^+$	1	2223	$3/2^+$	5	2530	$15/2^-$	4	3689	$35/2^-$	2
1782	$21/2^+$	2	2235	$9/2^+$	9	2531	$19/2^-$	2	4042	$29/2^+$	2
1784	$15/2^+$	3	2242	$5/2^-$	1	2536	$23/2^-$	1	4081	$33/2^+$	1
1798	$7/2^+$	4	2262	$7/2^+$	7	2537	$13/2^+$	9	4191	$31/2^+$	1
1802	$5/2^+$	4	2268	$11/2^-$	2	2543	$13/2^-$	4	4192	$39/2^+$	1
1806	$13/2^+$	3	2271	$3/2^-$	1	2548	$5/2^+$	9	4238	$35/2^+$	1
1822	$3/2^+$	2	2281	$19/2^-$	1	2550	$11/2^-$	4	4313	$33/2^+$	2
1823	$1/2^+$	1	2293	$11/2^+$	8	2551	$19/2^-$	3	4317	$35/2^+$	2
1841	$9/2^+$	6	2300	$9/2^+$	10	2559	$15/2^+$	7	4323	$31/2^+$	2
1846	$25/2^+$	1	2307	$5/2^+$	7	2564	$17/2^+$	6	4364	$37/2^+$	1
1846	$11/2^+$	5	2310	$17/2^-$	1	2567	$17/2^-$	4	4521	$37/2^+$	2
1862	$3/2^+$	3	2319	$7/2^+$	8	2574	$13/2^+$	10	5550	$39/2^-$	1

True,[27] for instance, derived TBME for the $0h_{9/2}^2$, $0h_{9/s}1f_{7/2}$, and $0h_{9/2}0i_{13/2}$ configurations from energy spectra and spectroscopic strengths of ^{210}Po. An extremely comprehensive study of the energy levels of ^{210}Po was recently made by Mann *et al.*[28] using the ^{209}Bi$(t,2n)^{210}$Po reaction. These results will allow more reliable and extensive evaluations of empirical TBME in this two proton system. Mann *et al.* proposed identifications of all members of the three configurations mentioned above as well as the $1f_{7/2}^2$ configuration. These identifications assume relatively little mixing between different configurations. This assumption is consistent with the predictions of the Kuo-Herling interaction. The KHP energy spectrum is compared to the results of Mann *et al.* in Table X. As is seen, there are candidates for all model states below 3.5 MeV. For each of the 3^-, 4^-, and 5^- states, one additional state is known experimentally below 3.5-MeV excitation. These extra states arise from particle-hole excitations such as $\nu 2p_{1/2}^{-1}1g_{9/2}$. An evaluation of the unperturbed E_x of the $0h_{9/2}0i_{13/2}$ $3^-, 4^-, 5^-$ states is difficult because of mixing with these low-lying particle-hole states. In Table X we show a tentative identification, after Schiffer and True,[27] which assumes the unperturbed $0h_{9/2}0i_{13/2}$ 3^- energy is that of the second 3^- state and the unperturbed 4^- and 5^- energies are the averages for the first two states of each spin.

The KHP energy spectrum of ^{212}Rn is compared to experiment in Table V and a more complete KHP spectrum is listed in Table XI. The experimental information of Table V is from a recent heavy-ion fusion-evaporation study by Stuchbery *et al.*[29] which considerably extended our knowledge of this nucleus, albeit for yrast and yrare states only. Stuchbery *et al.* also performed shell-model calculations in a space consisting of the three lowest proton orbits of the KHP space. They used an SDI residual interaction. Zwarts and Glaudemans[30] performed shell-model calculations in the complete KHP model space with both the Kuo-Herling interaction ($K_{\rm ph} = 1.0$) and an SDI interaction. These two studies provide a quite complete discussion of the spectroscopy of ^{212}Rn and we

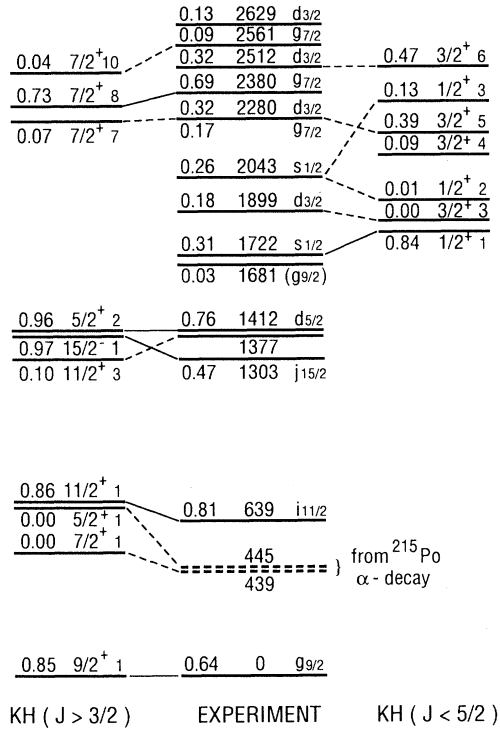

FIG. 2. The ^{210}Pb$(t,d)^{211}$Pb stripping results of Ellegaard, Barnes, and Flynn (Ref. 26) are shown in the center spectrum and the KHP model predictions are given in the two-side spectra. Spectroscopic factors are shown to the left in each spectrum and to the right is shown the orbit transferred for experiment or J^π k—where k orders the level by energy—for the predictions. For the experiment, the energy (in keV) of the states is listed in the middle. Five experimental levels—for which no orbit or S values were given—are omitted. All predicted levels for which $S > 0.02$ are included.

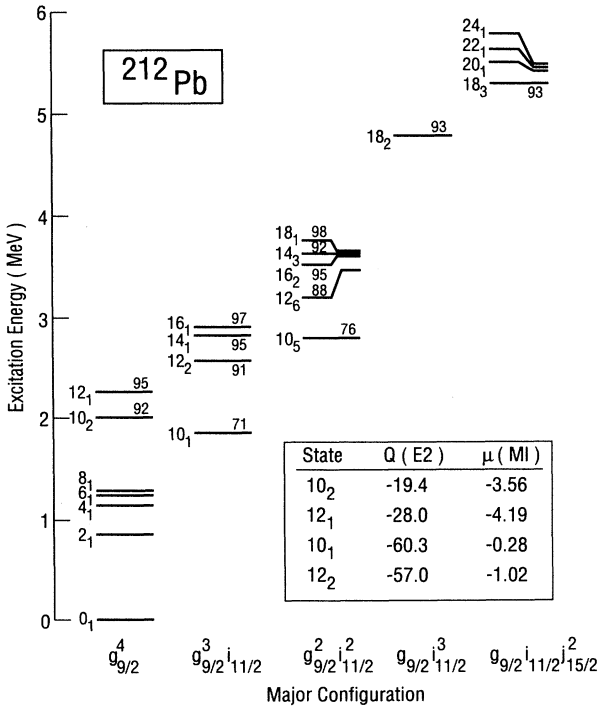

FIG. 3. Some predicted even-parity energy levels of ^{212}Pb. The levels are labeled by J_k^π—where k orders the levels by energy—and are sorted by the dominant configuration. Note only selected levels are shown and they are not necessarily the lowest in energy. The numbers on the levels are the percentage of the indicated configuration. The $J_k^\pi = 20_1^+ - 24_1^+$ levels are 100% $g_{9/2}i_{11/2}J_{15/2}^2$, the composition of the $J_k^\pi = 0_1^+ - 8_1^+$ $g_{9/2}^4$ levels is given in Table IX. The $Q(E2)$ and $\mu(M1)$ values are in e fm^2 and nuclear magnetons, respectively. The $Q(E2)$ were calculated with HO wave functions and $e_n = 1.0e$ while the $\mu(M1)$ were calculated with free-nucleon g factors.

TABLE VIII. KHP predictions for the even-parity energy spectrum of ^{212}Pb for $K_{\rm ph} = 1.07$. The index k orders states of a given J^π in energy. Levels with $k \leq 10$ are shown for $E_x < 3.0$ MeV while only k=1–2 levels are shown for $E_x > 3.0$ MeV.

E_x (keV)	J^π	k	E_x (keV)	J^π	k	E_x (keV)	J^π	k	E_x (keV)	J^π	k
0	0^+	1	2272	12^+	1	2665	4^+	10	2901	10^+	6
855	2^+	1	2275	3^+	3	2671	5^+	5	2903	16^+	1
1139	4^+	1	2287	2^+	6	2671	7^+	6	2908	12^+	3
1242	6^+	1	2343	8^+	4	2673	8^+	7	2931	5^+	10
1287	8^+	1	2344	9^+	3	2680	6^+	9	2944	7^+	10
1448	4^+	2	2361	4^+	6	2680	2^+	9	2946	3^+	10
1556	6^+	2	2420	7^+	3	2683	5^+	6	2949	11^+	3
1564	0^+	2	2435	6^+	5	2685	6^+	10	2967	12^+	4
1590	2^+	2	2463	2^+	7	2688	9^+	5	2978	13^+	2
1740	5^+	1	2467	5^+	3	2697	10^+	4	2980	0^+	6
1752	7^+	1	2472	0^+	4	2700	3^+	6	2980	15^+	1
1823	1^+	1	2475	4^+	7	2730	7^+	7	2991	9^+	7
1827	4^+	3	2483	6^+	6	2742	8^+	8	3113	14^+	2
1861	3^+	1	2488	5^+	4	2742	5^+	7	3656	18^+	1
1873	10^+	1	2502	7^+	4	2758	3^+	7	3669	16^+	2
1887	2^+	3	2511	1^+	2	2768	8^+	9	3821	15^+	2
1891	3^+	2	2524	4^+	8	2771	7^+	8	3855	17^+	1
1893	4^+	1	2544	8^+	5	2785	11^+	2	4759	18^+	2
1903	2^+	4	2555	2^+	8	2786	10^+	5	4833	17^+	2
1915	0^+	3	2565	7^+	5	2803	2^+	10	5442	20^+	1
1934	4^+	4	2573	6^+	7	2804	3^+	8	5453	22^+	1
1935	6^+	3	2575	3^+	4	2809	8^+	10	5480	19^+	1
1937	7^+	2	2577	12^+	2	2819	1^+	4	5498	20^+	2
1944	5^+	2	2580	4^+	9	2820	9^+	6	5507	19^+	2
1947	8^+	2	2581	11^+	1	2822	5^+	8	5526	24^+	1
1964	6^+	4	2595	3^+	5	2823	0^+	5	5543	23^+	1
2007	10^+	2	2596	10^+	3	2829	14^+	1	5546	21^+	1
2008	8^+	3	2607	6^+	8	2840	3^+	9	5591	22^+	2
2105	9^+	2	2622	8^+	6	2853	13^+	1	5616	21^+	2
2231	2^+	5	2635	9^+	4	2891	5^+	9	5878	24^+	2
2251	4^+	5	2636	1^+	3	2901	7^+	9	5954	23^+	2

make only a few comments. Stuchbery *et al.* list the configurational composition they found with the SDI for some of the even-parity levels. Their results for the 0^+–8^+ even-J levels shows a "collective" structure similar to the KHP predictions shown in Table XII but with lessened mixing; they report $\sim$ 76% $0h^4_{9/2}$ as opposed to the $\sim$62% found with the KHP interaction. Predictions for quadrupole moments and $B(E2)$ values for the 0^+–8^+ states are given in Table XII. The effective charge used was that which gave an average best agreement with the three experimental values shown. The very low value of the necessary increment to the proton charge—0.27e—is an indication that the KHP model space is adequate for a detailed description of these levels.

An improvement on the KHP interaction could quite likely be had by modifications designed to better repro-

TABLE IX. KHP predictions for the energies, configurations, $B(E2)$ values (for decay to the next lower state) and quadrupole moments of the ground-state band of ^{212}Pb. $B(E2)$ and $Q(E2)$ were calculated with an effective charge of 1.0e using WS parameters which give an rms neutron radius of 5.694 fm. The four most prominent configurations are listed.

J^π	E_x (keV)		Configuration (%)				$B(E2)$	$Q(E2)$
	KHP	Expt	$g^4_{9/2}$	$g^2_{9/2}i^2_{11/2}$	$g^2_{9/2}j^2_{15/2}$	$g^3_{9/2}d_{5/2}$	(e^2 fm^4)	(e fm^2)
0^+	0	0	43.3	25.4	11.9	0.1		
2^+	855	805	62.0	17.5	8.6	2.4	231.7	− 0.55
4^+	1139	1117	66.8	16.6	8.1	0.9	75.7	− 1.65
6^+	1242	1277	68.4	16.4	8.1	0.4	29.4	− 7.8
8^+	1287	1335	69.0	16.4	8.0	0.2	8.5	−19.5

TABLE X. The KHP energy spectrum of ^{210}Po for K_{ph}=0.92. ΔE_x is experiment−model and is positive if the model prediction is too bound. The energy entry for the ground state is the binding energy relative to ^{208}Pb. All model levels are listed for E_x < 3.8 MeV while only the first three of each spin parity are listed for E_x >3.8 MeV. Experimental energies preceded by an asterisk are not included in the averaging.

Model			Expt		Dominant
E_x	J^π	No.	E_x	ΔE_x	conf.
−8810	0^+	1	−8782	+28	$0h_{9/2}^2$
1199	2^+	1	1181	−18	$0h_{9/2}^2$
1465	4^+	1	1427	−38	$0h_{9/2}^2$
1481	6^+	1	1473	− 8	$0h_{9/2}^2$
1532	8^+	1	1557	+25	$0h_{9/2}^2$
2124	8^+	2	2188	+64	$0h_{9/2}1f_{7/2}$
2318	1^+	1	2394	+76	$0h_{9/2}1f_{7/2}$
2328	6^+	2	2326	− 2	$0h_{9/2}1f_{7/2}$
2355	7^+	1	2438	+83	$0h_{9/2}1f_{7/2}$
2369	2^+	2	2290	−79	$0h_{9/2}1f_{7/2}$
2396	5^+	1	2403	+ 7	$0h_{9/2}1f_{7/2}$
2400	3^+	1	2414	+14	$0h_{9/2}1f_{7/2}$
2431	4^+	2	2383	−48	$0h_{9/2}1f_{7/2}$
2644	0^+	2	2609	−35	$1f_{7/2}^2$
2675	11^-	1	2849	+174	$0h_{9/2}0i_{13/2}$
2923	2^+	3	*2868	−55	$1f_{7/2}^2$
2927	2^-	1	3024	+97	$0h_{9/2}0i_{13/2}$
2957	9^-	1	3000	+43	$0h_{9/2}0i_{13/2}$
2998	3^-	1	2846	−152	$0h_{9/2}0i_{13/2}$
3024	8^-	1	3138	+114	$0h_{9/2}0i_{13/2}$
3025	7^-	1	3016	− 9	$0h_{9/2}0i_{13/2}$
3041	10^-	1	3183	+142	$0h_{9/2}0i_{13/2}$
3073	6^-	1	3125	+52	$0h_{9/2}0i_{13/2}$
3097	5^-	1	*2968	−129	$0h_{9/2}0i_{13/2}$
3097	4^-	1	*3093	− 4	$0h_{9/2}0i_{13/2}$
3179	4^+	3	3094	−85	$1f_{7/2}^2$
3248	6^+	3	3219	−29	$1f_{7/2}^2$
3577	3^-	2			
3865	5^-	2			
3892	7^-	2	$\langle\Delta E_x\rangle_{rms}$= 67 keV		
3928	9^-	2			
3976	4^-	2	$\langle\Delta E_B\rangle$= 49 keV		
4049	6^-	2			
4052	8^-	2			
4089	10^-	2			
4344	3^+	2			
4366	7^+	2			
4370	5^+	2			
4539	0^+	3			
4644	3^+	3			
4649	5^+	3			
4658	8^+	3			
4674	10^+	1			
5210	1^+	2			
5681	9^-	3			
5833	7^-	3			
5880	5^-	3			
5897	4^-	3			
5911	8^-	3			
5948	6^-	3			
7468	1^+	3			

duce the spectra of the two- and four-proton systems. The predictions for the even-parity states shown in Tables X, XI, and XII are really quite good. The predictions involving the unique-parity $\pi 0i_{13/2}$ orbit are not so good; the odd-parity states are too bound. Use of a less bound $\pi 0i_{13/2}$ orbit would give improved agreement with experiment. Even better agreement would result from an adjustment of the $0h_{9/2}0i_{13/2}$ TBME such that the average value is ~100 keV more positive. This discrepancy is in qualitative agreement with that expected from the octupole coupling to core-excited neutron states, which is discussed by Poletti *et al.*[21] Another possible contributing factor is discussed in Sec. V.

C. ^{210}Bi

A comprehensive study of ^{210}Bi via the ^{209}Bi$(n,\gamma)^{210}$Bi reaction has recently been made by Ponting *et al.*[31] using the Los Alamos Omega West thermal neutron facility. These authors proposed identification of all states of the first six odd-parity configurations, the first even-parity configuration, and six of ten states of the second even-parity configuration of ^{210}Bi. The ordering of the configurations composed of a proton in orbit $j\pi$ and a neutron in orbit $i\nu$ is according to the zeroth-order expression

$$E_{ij} = \epsilon_{j\pi} + \epsilon_{i\nu} + 7736 \text{ keV} , \quad (6)$$

where, as can be inferred from Fig. 1, −7736 keV is the zeroth-order binding energy of the $\pi 0h_{9/2}\nu 1g_{9/2}$ con-

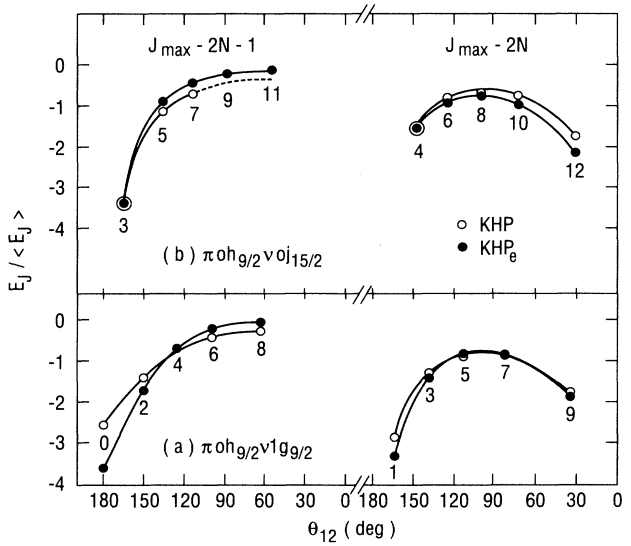

FIG. 4. Normalized $\pi 0h_{9/2}\nu 1g_{9/2}$ TBME (bottom) and unnormalized $0h_{9/2}0j_{15/2}$ TBME (top) plotted against the angle Θ_{12} between $\mathbf{j_1}$ and $\mathbf{j_2}$. $\langle E_J\rangle$ and Θ_{12} are defined in the text as are the KHP and KHP$_e$ configurations. The TBME are labeled by J.

TABLE XI. KHP predictions for the energy spectrum of ^{212}Rn for $K_{ph} = 0.92$. The index k orders states of a given J^π in energy. Levels with $k \leq 10$ are shown for $E_x < 3523$ keV while only k=1–2 levels are shown for $E_x > 3523$ keV.

E_x (keV)	J^π	k	E_x (keV)	J^π	k	E_x (keV)	J^π	k	E_x (keV)	J^π	k
0	0^+	1	2873	8^-	1	3328	9^+	3	3824	13^-	2
1333	2^+	1	2874	3^-	1	3348	6^+	8	3834	16^-	1
1560	4^+	1	2936	5^-	1	3374	7^+	5	3839	12^-	2
1646	6^+	1	2937	7^+	3	3382	3^+	5	3915	0^-	1
1667	8^+	1	2959	12^+	1	3385	1^+	3	3923	14^-	2
2110	8^+	2	2959	4^-	1	3386	5^+	6	3926	14^+	2
2275	6^+	2	2965	4^+	5	3388	10^+	3	3927	1^-	1
2287	4^+	2	3041	6^+	5	3398	6^+	9	3940	2^-	2
2299	7^+	1	3050	0^+	4	3401	8^+	6	3973	15^-	2
2316	1^+	1	3063	1^+	2	3410	7^+	6	4115	1^-	2
2344	5^+	1	3076	6^+	6	3415	4^+	9	4128	13^+	2
2354	2^+	2	3085	2^+	5	3423	5^+	7	4373	17^-	2
2368	3^+	1	3104	10^+	2	3431	10^-	2	4416	18^-	1
2380	4^+	3	3133	5^+	3	3433	13^+	1	4505	16^-	2
2396	6^+	3	3142	6^-	2	3463	6^+	10	4918	20^+	1
2431	2^+	3	3145	3^-	2	3472	11^+	2	4928	0^-	2
2453	0^+	2	3147	5^+	4	3484	5^+	8	4966	18^+	1
2545	7^+	2	3154	4^+	6	3497	4^+	10	4992	16^+	1
2547	5^+	2	3157	9^+	2	3497	8^+	7	5176	17^+	1
2585	11^-	1	3161	3^+	3	3501	9^+	4	5189	19^+	1
2655	4^+	4	3204	6^+	7	3512	3^+	6	5219	18^+	2
2679	3^+	2	3227	8^+	4	3522	2^+	8	5223	16^+	2
2716	2^+	4	3235	3^+	4	3525	9^-	2	5243	15^+	1
2728	6^+	4	3242	2^+	6	3544	5^-	2	5257	15^+	2
2730	0^+	3	3257	5^+	5	3561	13^-	1	5259	17^+	2
2732	10^+	1	3266	4^+	7	3571	7^-	2	6123	19^+	2
2754	8^+	3	3278	8^+	5	3616	4^-	2	6126	20^+	2
2800	9^-	1	3285	2^+	7	3642	12^-	1	6756	21^-	1
2836	9^+	1	3287	14^+	1	3645	8^-	2	6773	19^-	1
2847	2^-	1	3288	4^+	8	3672	11^-	2	6804	18^-	2
2858	10^-	1	3288	7^+	4	3761	17^-	1	6954	20^-	1
2861	7^-	1	3305	12^+	2	3767	15^-	1	7237	19^-	2
2871	6^-	1	3321	11^+	1	3777	14^-	1	8697	20^-	2

figuration. The ordering is listed in Table XIII and the low-lying spectrum of ^{210}Bi, with the experimental states and proposed configurational assignments of Ponting *et al.*,[31] is compared to the KHP predictions in Table XIV. The identifications of Ponting *et al.* are based on previous evidence, γ-ray branching, and also—very strongly—on shell-model expectations. It is quite probable that some of them are wrong. For instance, we have indicated in Table XIV that possible high-spin even-parity states—previously proposed at ~1801, ~1812, and ~ 1987 keV[7]—are not included in the Ponting spectrum. Nevertheless, the assignments for the three low-

TABLE XII. KHP predictions for the energies, configurations, $B(E2)$ values (for decay to the next lower state) and quadrupole moments of the ground-state band of ^{212}Rn. The B(E2) and $Q(E2)$ are in e^2 fm^4 and e fm^2, respectively, and were calculated with an effective charge of 1.27e using WS parameters which give a rms charge radius of 5.56 fm. The three most prominent configurations are listed.

J^π	E_x (keV)		Configuration (%)			$B(E2)$		$Q(E2)$
	KHP	Expt	$h^4_{9/2}$	$h^2_{9/2}i^2_{13/2}$	$h^2_{9/2}f^2_{7/2}$	KHP	Expt	KHP
0^+	0	0	41.8	23.2	20.1			
2^+	1333	1274	59.7	17.3	16.5	256.8		+ 6.1
4^+	1560	1501	63.8	16.2	15.5	61.4	79(3)	+ 6.5
6^+	1646	1640	62.3	16.9	16.7	34.9	30(4)	− 4.5
8^+	1667	1694	64.6	16.5	15.2	10.5	9.8(8)	−23.3

TABLE XIII. Zeroth-order configurational energies for KHP states of ^{210}Bi.

Orbits		Relative energy
π	ν	(MeV)
$0h_{9/2}$	$1g_{9/2}$	0.00
$0h_{9/2}$	$0i_{11/2}$	0.78
$1f_{7/2}$	$1g_{9/2}$	0.90
$0h_{9/2}$	$0j_{15/2}$	1.42
$0h_{9/2}$	$2d_{5/2}$	1.57
$0i_{13/2}$	$1g_{9/2}$	1.61
$1f_{7/2}$	$0i_{11/2}$	1.68

est odd-parity configurations and all $0h_{9/2}0j_{15/2}$ states other than 9^+ and 11^+ states appear quite reliable, and we have taken on the exercise of varying selected KHP TBME in order to obtain agreement with the proposed spectrum of Ponting *et al.*[31] The aim was to reproduce all the $E_x < 2$ MeV states and some selected higher-lying states. All experimental states listed in Table XIV were reproduced except those for which the associated model states are marked with an asterisk. The modified TBME, obtained as described in the next paragraph, are listed in Table XV.

With the KHP interaction, the yrast 0^- through 9^- states of ^{210}Bi are all >96% $\pi h_{9/2}\nu g_{9/2}$. The identification of these states is certain and the modification of the KHP TBME to reproduce the experimental energies straightforward. The next two odd-parity configurations (see Table XIII) are strongly mixed with each other but not with others. This is also true for the fourth and fifth odd-parity configurations. Our method of handling strongly mixed configurations was to change both diagonal TBME for a particular J by the same amount so as to reproduce the average of the two experimental energies with which the two states are identified. Then the energies of the two were matched by varying the off-diagonal

TABLE XIV. The KH energy spectrum of ^{210}Bi for $K_{\rm ph}$=0.90. ΔE_x is experiment − model and is positive if the model prediction is too bound. The energy entry for the ground state is the binding energy relative to ^{208}Pb. All experimental levels are listed for $E_x < 2.0$ MeV while all model levels are included which belong predominantly to the three odd-parity configurations and the two even-parity configurations which are lowest in zeroth order. The TBME corresponding to the model energies preceded by an asterisk were not modified.

Experiment			Model		Dominant	Experiment			Model		Dominant
E_x	J^π	No.	E_x	ΔE_x	conf.	E_x	J^π	No.	E_x	ΔE_x	conf.
−8403	1^-	1	−8380	−23	$0h_{9/2}1g_{9/2}$	1479	9^-	2	1511	+168	$0h_{9/2}0i_{11/2}$
47	0^-	1	−84	+131	$0h_{9/2}1g_{9/2}$	1523	4^+	1	1570	− 47	$0h_{9/2}0j_{15/2}$
271	9^-	1	291	−20	$0h_{9/2}1g_{9/2}$	1531	2^+	1	1827	−296	$0i_{13/2}1g_{9/2}$
320	2^-	1	272	+48	$0h_{9/2}1g_{9/2}$	1585	2^-	4	1612	− 27	$1f_{7/2}0i_{11/2}$
348	3^-	1	347	+ 1	$0h_{9/2}1g_{9/2}$	1706	5^+	1	1756	− 50	$0h_{9/2}0j_{15/2}$
433	7^-	1	453	−20	$0h_{9/2}1g_{9/2}$	1753	10^+	1	1725	+28	$0h_{9/2}0j_{15/2}$
439	5^-	1	454	−15	$0h_{9/2}1g_{9/2}$	1776	6^+	1	1761	+ 15	$0h_{9/2}0j_{15/2}$
503	4^-	1	497	+ 6	$0h_{9/2}1g_{9/2}$	1794	8^+	1	1790	+ 4	$0h_{9/2}0j_{15/2}$
550	6^-	1	579	−29	$0h_{9/2}1g_{9/2}$	1801		possible $(9\text{-}11)^+$; Ref. 7			
563	1^-	2	653	−90	$0h_{9/2}0i_{11/2}$	1812		possible $(8\text{-}11)^+$; Ref. 7			
583	8^-	1	615	−32	$0h_{9/2}1g_{9/2}$	1837	7^+	1	1911	−74	$0h_{9/2}0j_{15/2}$
670	10^-	1	864	−195	$0h_{9/2}0i_{11/2}$	1897	9^-	3	2050	−153	$1f_{7/2}0i_{11/2}$
916	8^-	2	986	−70	$1f_{7/2}1g_{9/2}$	1897	3^+	2	2096	−199	$0i_{13/2}1g_{9/2}$
972	2^-	2	972	− 0	$0h_{9/2}0i_{11/2}$	1925	2^-	5	1908	+ 17	$0h_{9/2}2d_{5/2}$
994	3^+	1	1094	−100	$0h_{9/2}0j_{15/2}$	1980	7^-	4	2003	− 23	$0h_{9/2}2d_{5/2}$
1165	1^-	3	1216	−51	$1f_{7/2}1g_{9/2}$	1985	3^-	4	2023	− 38	$1f_{7/2}0i_{11/2}$
1175	2^-	3	1230	−55	$1f_{7/2}1g_{9/2}$	1987		possible $(9\text{-}11)^+$; Ref. 7			
1184	8^-	3	1357	−173	$0h_{9/2}0i_{11/2}$	1990	3^-	5	2043	−53	$0h_{9/2}2d_{5/2}$
1208	6^-	2	1345	−137	$1f_{7/2}1g_{9/2}$	2006	4^+	2	*2149	−143	$0i_{13/2}1g_{9/2}$
1248	4^-	2	1360	−112	$0h_{9/2}0i_{11/2}$	2015	6^+	2	*2203	−188	$0i_{13/2}1g_{9/2}$
1301	7^-	2	1324	−23	$0h_{9/2}0i_{11/2}$	2026	1^+	1	1929	+ 97	$0i_{13/2}0i_{11/2}$
1316	11^+	1	1652	−336	$0i_{13/2}1g_{9/2}$	2072	9^+	1	*1947	+125	$0h_{9/2}0j_{15/2}$
1336	5^-	2	1281	+ 55	$0h_{9/2}0i_{11/2}$	2100	11^+	2	*2031	+ 69	$0h_{9/2}0j_{15/2}$
1339	6^-	3	1437	− 98	$0h_{9/2}0i_{11/2}$	2259	7^+	2	*2169	+ 90	$0i_{13/2}1g_{9/2}$
1374	3^-	2	1154	+220	$0h_{9/2}0i_{11/2}$		9^+	2	*2100		$0i_{13/2}1g_{9/2}$
1383	7^-	3	1448	−65	$1f_{7/2}1g_{9/2}$		5^+	2	*2178		$0i_{13/2}1g_{9/2}$
1390	4^-	3	1413	−24	$1f_{7/2}1g_{9/2}$		8^+	2	*2225		$0i_{13/2}1g_{9/2}$
1463	5^-	3	1438	+ 25	$1f_{7/2}1g_{9/2}$		10^+	2	*2237		$0i_{13/2}1g_{9/2}$
1469	12^+	1	1431	+38	$0h_{9/2}0j_{15/2}$	2733	14^-	1	3137	−404	$0i_{13/2}0j_{11/2}$
1476	3^-	3	1399	+77	$1f_{7/2}1g_{9/2}$						

TBME between them. Some iteration is necessary. The modified pn interaction was combined with the $\Delta^{(\alpha)} \neq 0$ interaction discussed at the end of Sec. III and the resultant was labeled KHP$_e$.

The relationship between the KHP and modified (KHP$_e$) pn TBME was examined to look for possible regularities. We first consider the $0h_{9/2}1g_{9/2}$ configuration. The levels of this configuration provide a classic example of the systematic behavior of the TBME of nonequivalent particles.[32] In Fig. 4 we compare the KHP and KHP$_e$ TBME for this multiplet using the clarifying method of display introduced by Schiffer.[32] Since the states in question are dominated so strongly by $0h_{9/2}1g_{9/2}$, the KHP$_e$ set is essentially equivalent to varying the $\pi 0h_{9/2}\nu 1g_{9/2}$ TBME and leaving the other KHP TBME unchanged and is very close to the set resulting from an assumption of a pure $\pi 0h_{9/2}\nu 1g_{9/2}$ configuration. The average energy, $\langle E_J \rangle$, and Θ_{12} in Fig. 4 are defined as

$$\langle E_J \rangle = \text{abs}\left[\frac{\sum_J (2J+1)\langle j_1 j_2 | V | j_1 j_2 \rangle_J}{\sum_J (2J+1)}\right] , \tag{7}$$

$$\Theta_{12} = \cos^{-1}\left\{\frac{J(J+1) - j_1(j_1+1) - j_2(j_2+1)}{2[j_1(j_1+1)j_2(j_2+1)]^{1/2}}\right\} . \tag{8}$$

A similar comparison for the known (i.e., all but 9^+ and 11^+) states of the even-parity $0h_{9/2}0j_{15/2}$ configuration is shown in the upper half of Fig. 4. A striking feature of Fig. 4 is that not only do the Kuo-Herling TBME exhibit smoothly varying behavior, but the empirical TBME do also. All the Kuo-Herling multiplets exhibit this smooth pattern as do more schematic representations of the interaction such as the SDI. If we assume a smoothly varying behavior for the odd J states of the $0h_{9/2}0j_{15/2}$ multiplet, we infer an extrapolation such as the dashed line in the upper left panel of Fig. 4. This leads to predictions for the excitation energies of the 9_1^+ and 11_2^+ states of 1878 and 1955 keV which are 69 and 76 keV, respectively, below the KHP predictions of Table XIV and not too far from the E_x of the three possible high-spin states listed as such in Table XIV. However, as is seen from a perusal of the Δ column of Table XV, not all the of the empirical TBME are so smoothly varying. Note, for example, the stagger of Δ for the odd J TBME of the $0h_{9/2}0i_{11/2}$ multiplet.

Because the KHP and KHP$_e$ curves of Fig. 4 are not too dissimilar, a convenient measure of the difference in magnitude of the two sets of TBME is provided by the $\langle E_J \rangle$. For the $\pi 0h_{9/2}\nu 1g_{9/2}$ and $\pi 0h_{9/2}\nu 0j_{15/2}$ sets the empirical KHP$_e$ interaction gives values of $\langle E_J \rangle$ larger than the KHP interaction by 20% and 17%, respectively. The possible significance of these differences will be discussed in Sec. V.

D. ^{212}At

The high-spin spectroscopy of ^{212}At was investigated via the ^{208}Pb(^{7}Li,3n)^{212}At reaction by Sjoreen *et al.*[33] A

TABLE XV. The modified TBME of the KHP$_e$ interaction compared to the original KHP TBME for $K_{\text{ph}} = 0.90$. The TBME have the form $\langle ij|V|km\rangle$ with the orbits i, j, k, m as listed. The TBME are in MeV. In the last column, Δ is KHP − KHP$_e$ in MeV.

Orbits $i\ j$	Orbits $k\ m$	J	$\langle ij\|V\|km\rangle$ KHP	KHP$_e$	Δ
$0h_{9/2}1g_{9/2}$	$0h_{9/2}1g_{9/2}$	0	−0.6595	−0.5480	−0.1115
$0h_{9/2}1g_{9/2}$	$0h_{9/2}1g_{9/2}$	1	−0.5934	−0.6149	+0.0215
$0h_{9/2}1g_{9/2}$	$0h_{9/2}1g_{9/2}$	2	−0.3130	−0.2862	−0.0268
$0h_{9/2}1g_{9/2}$	$0h_{9/2}1g_{9/2}$	3	−0.2458	−0.2690	+0.0232
$0h_{9/2}1g_{9/2}$	$0h_{9/2}1g_{9/2}$	4	−0.1140	−0.1314	+0.0174
$0h_{9/2}1g_{9/2}$	$0h_{9/2}1g_{9/2}$	5	−0.1488	−0.1867	+0.0379
$0h_{9/2}1g_{9/2}$	$0h_{9/2}1g_{9/2}$	6	−0.0422	−0.0956	+0.0534
$0h_{9/2}1g_{9/2}$	$0h_{9/2}1g_{9/2}$	7	−0.1494	−0.1920	+0.0426
$0h_{9/2}1g_{9/2}$	$0h_{9/2}1g_{9/2}$	8	−0.0084	−0.0620	+0.0536
$0h_{9/2}1g_{9/2}$	$0h_{9/2}1g_{9/2}$	9	−0.3382	−0.3810	+0.0428
$0h_{9/2}0i_{11/2}$	$0h_{9/2}0i_{11/2}$	1	−0.3973	−0.4983	+0.1010
$0h_{9/2}0i_{11/2}$	$0h_{9/2}0i_{11/2}$	2	−0.2043	−0.2608	+0.0565
$0h_{9/2}0i_{11/2}$	$0h_{9/2}0i_{11/2}$	3	−0.1478	−0.0153	−0.1325
$0h_{9/2}0i_{11/2}$	$0h_{9/2}0i_{11/2}$	4	+0.0105	−0.0325	+0.0430
$0h_{9/2}0i_{11/2}$	$0h_{9/2}0i_{11/2}$	5	−0.0987	−0.0597	−0.0390
$0h_{9/2}0i_{11/2}$	$0h_{9/2}0i_{11/2}$	6	+0.0332	−0.0878	+0.1210
$0h_{9/2}0i_{11/2}$	$0h_{9/2}0i_{11/2}$	7	−0.0771	−0.1181	+0.0410
$0h_{9/2}0i_{11/2}$	$0h_{9/2}0i_{11/2}$	8	−0.0445	−0.2505	+0.2060
$0h_{9/2}0i_{11/2}$	$0h_{9/2}0i_{11/2}$	9	−0.1068	+0.0422	−0.1490
$0h_{9/2}0i_{11/2}$	$0h_{9/2}0i_{11/2}$	10	−0.5566	−0.7746	+0.2180
$0h_{9/2}0i_{11/2}$	$1f_{7/2}1g_{9/2}$	1	−0.1939	−0.2179	+0.0240
$0h_{9/2}0i_{11/2}$	$1f_{7/2}1g_{9/2}$	2	+0.0697	+0.0357	+0.0340
$0h_{9/2}0i_{11/2}$	$1f_{7/2}1g_{9/2}$	3	−0.0674	+0.0341	−0.1015
$1f_{7/2}1g_{9/2}$	$1f_{7/2}1g_{9/2}$	1	−0.4019	−0.5029	+0.1010
$1f_{7/2}1g_{9/2}$	$1f_{7/2}1g_{9/2}$	2	−0.1977	−0.2542	+0.0565
$1f_{7/2}1g_{9/2}$	$1f_{7/2}1g_{9/2}$	3	−0.1545	−0.0225	−0.1320
$1f_{7/2}1g_{9/2}$	$1f_{7/2}1g_{9/2}$	4	−0.0705	−0.2215	+0.1510
$1f_{7/2}1g_{9/2}$	$1f_{7/2}1g_{9/2}$	5	−0.0948	−0.1008	+0.0060
$1f_{7/2}1g_{9/2}$	$1f_{7/2}1g_{9/2}$	6	−0.1155	−0.2855	+0.1700
$1f_{7/2}1g_{9/2}$	$1f_{7/2}1g_{9/2}$	7	−0.0832	−0.1802	+0.0970
$1f_{7/2}1g_{9/2}$	$1f_{7/2}1g_{9/2}$	8	−0.5326	−0.6226	+0.0900
$0h_{9/2}0j_{15/2}$	$0h_{9/2}0j_{15/2}$	3	−0.9022	−1.0248	+0.1226
$0h_{9/2}0j_{15/2}$	$0h_{9/2}0j_{15/2}$	4	−0.4008	−0.4766	+0.0758
$0h_{9/2}0j_{15/2}$	$0h_{9/2}0j_{15/2}$	5	−0.2492	−0.3274	+0.0782
$0h_{9/2}0j_{15/2}$	$0h_{9/2}0j_{15/2}$	6	−0.2359	−0.2447	+0.0089
$0h_{9/2}0j_{15/2}$	$0h_{9/2}0j_{15/2}$	7	−0.1183	−0.2233	+0.1050
$0h_{9/2}0j_{15/2}$	$0h_{9/2}0j_{15/2}$	8	−0.2088	−0.2278	+0.0190
$0h_{9/2}0j_{15/2}$	$0h_{9/2}0j_{15/2}$	10	−0.2533	−0.2483	−0.0050
$0h_{9/2}0j_{15/2}$	$0h_{9/2}0j_{15/2}$	12	−0.5672	−0.5522	−0.0150
$0h_{9/2}2d_{5/2}$	$0h_{9/2}2d_{5/2}$	2	−0.4338	−0.4632	+0.0294
$0h_{9/2}2d_{5/2}$	$0h_{9/2}2d_{5/2}$	3	−0.1543	−0.2313	+0.0770
$0h_{9/2}2d_{5/2}$	$0h_{9/2}2d_{5/2}$	7	−0.1968	−0.2438	+0.0470
$0h_{9/2}2d_{5/2}$	$1f_{7/2}0i_{11/2}$	2	+0.1279	+0.1549	−0.0270
$0h_{9/2}2d_{5/2}$	$1f_{7/2}0i_{11/2}$	3	+0.0129	−0.0001	+0.0130
$0i_{13/2}1g_{9/2}$	$0i_{13/2}1g_{9/2}$	2	−0.3653	−0.7113	+0.3460
$0i_{13/2}1g_{9/2}$	$0i_{13/2}1g_{9/2}$	3	−0.1568	−0.3858	+0.2290
$0i_{13/2}1g_{9/2}$	$0i_{13/2}1g_{9/2}$	11	−0.4589	−0.8679	+0.4090
$1f_{7/2}0i_{11/2}$	$1f_{7/2}0i_{11/2}$	2	−0.5895	−0.6189	+0.0294
$1f_{7/2}0i_{11/2}$	$1f_{7/2}0i_{11/2}$	3	−0.2491	−0.3181	+0.0690
$1f_{7/2}0i_{11/2}$	$1f_{7/2}0i_{11/2}$	9	−0.2780	−0.4610	+0.1830
$0i_{13/2}0i_{11/2}$	$0i_{13/2}0i_{11/2}$	1	−1.1013	−1.0273	−0.0740
$0i_{13/2}0j_{11/2}$	$0i_{13/2}0j_{11/2}$	14	−0.6230	−0.9640	+0.3410

TABLE XVI. Magnetic moments (in nm) for the yrast 11^+ and 15^- states of ^{212}At. The experimental results are from Sjoreen *et al.* (Ref. 33). KHP and KHP$_e$ predictions are given utilizing the theoretical effective operators of Arima *et al.* (Ref. 34) and the semiempirical operators described in the text.

	Expt	Arima			Semiemp		
J^π		KHP	KHP$_e$	pure[a]	KHP	KHP$_e$	pure[b]
11^+	5.95	6.16	7.06	8.06	5.74	6.59	7.57
15^-	9.33	8.79	8.84	6.01	8.62	8.64	5.87

[a] $\pi(h^2_{9/2}i_{13/2})\nu g_{9/2}$ for the 11^+ state. There are 25 11^+ states in this configuration and thus $\mu(11^+)$ is complex, the value listed is for KHP$_e$. For $\pi h^2_{9/2}$ coupled to 0^+, $\mu(11^+) = \mu(\pi i_{13/2}) + \mu(\nu g_{9/2})$, which is, e.g., 6.73 nm for the semiempirical operators.
[b] $\pi h^3_{9/2}\nu g_{9/2}$ for the 15^- state which is unique.

comparison of these results and diagonalized shell-model predictions has not been made heretofore. It was proposed by Sjoreen *et al.* that the high-spin level scheme they observed was built on the 9^-_1 level. We were able to diagonalize the ^{212}At states with $J \geq 9$ only, but this is sufficient to compare to the experimental results of Sjoreen *et al.* Both the KHP and KHP$_e$ results are compared to the level scheme proposed by Sjoreen *et al.*[33] in Fig. 5. Our predictions certainly support their spin-parity assignments. It is noteworthy that the KHP$_e$ interaction is in considerably better agreement with their excitation energies than the KHP interaction, particularly for the 11^+_1 state. As seen in Table XV, the KHP$_e$ J=11 $0i_{13/2}1g_{9/2}$ TBME, which has a strong effect on this energy, differs the most from the KHP interaction.

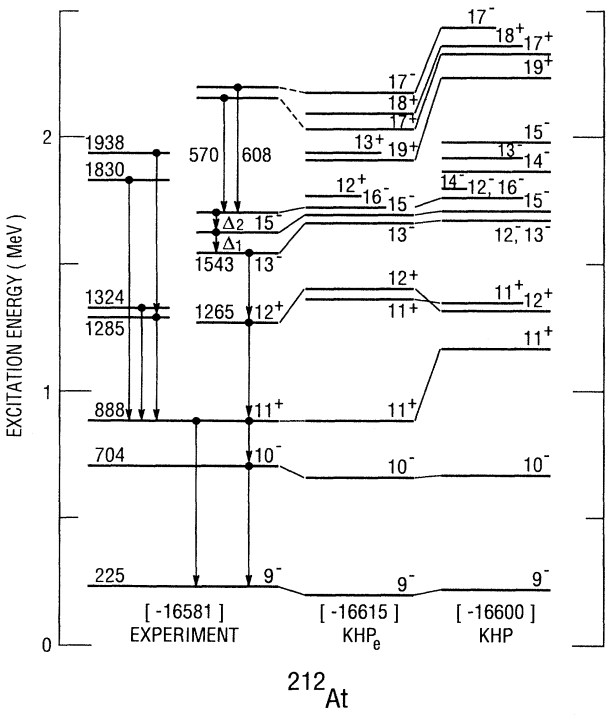

FIG. 5. Comparison of the experimental high-spin results of Sjoreen *et al.* (Ref. 33) for ^{212}At to the KHP$_e$ and KHP predictions for $K_{\rm ph} = 0.90$. Energies are in keV. The numbers in square brackets are the binding energies relative to ^{208}Pb. The experimental spin parities are those proposed by Sjoreen *et al.* The speculated identifications for the levels above the 15^- level are ours. Only model states that are deemed of possible interest are shown.

Sjoreen *et al.* did not observe a $15^- \rightarrow 13^-$ transition and proposed a transition energy of less than 95 keV to explain this nonobservation and the 54 ns mean life of the 15^- level. The KHP$_e$ and KHP predictions for this transition energy are 37 and 41 keV, respectively, consistent with their inference. Sjoreen *et al.* placed the 570 and 608 γ transitions of their Fig. XV above the 15^- level and speculated that they might feed a 16^- level close enough to the 15^- level so that the $16^- \rightarrow 15^-$ transition would be unobserved (note that there is no experimental evidence for this "missing" transition). The predictions support this speculation since we find KHP$_e$ and KHP $16^- \rightarrow 15^-$ transition energies of 23 and 50 keV, respectively. Finally, the assumption of an intermediate 16^- state allows us to propose 17^+ and 17^- for the states decaying by 570 and 608 keV radiations, i.e., both of these transitions have prompt components[33] which would not be the case if 17^+ and 17^- states decayed to a 15^- state with transition energies of ~600 keV. It is clear from Fig. 5 that the 19^+_1 state should be isomeric. Sjoreen *et al.* estimated a mean lifetime of $\sim$ 14 μsec for a $19^+ \rightarrow 16^-$ $E3$ transition, but, due to the low angular momentum brought in by the ^{7}Li beam, expected only a weak formation of this high-spin state. They did not observe any evidence for such an isomer.

Sjoreen *et al.* measured the magnetic moments of the 11^+ and 15^- states. A first step in the calculation of shell-model predictions for magnetic moments or $M1$ transitions is to choose the relevant operators. It is known that the free-nucleon g factors are inadequate in the lead region. We have chosen to use the effective operators derived from fundamental considerations for orbits in the lead region by Arima *et al.*[34] These may not reproduce experiment as well as empirical effective g factors but we do have the secondary motive of testing fundamental predictions for these operators. The operators we use are obtained by applying the corrections to the

TABLE XVII. Dominant configurational contributions to the wave functions of the yrast KHP_e and KHP 11^+ and 15^- states of ^{212}At.

State	Configuration	Percentage	
		KHP_e	KHP
11^+	$1h^2_{9/2}0i_{13/2}1g_{9/2}$	70.1	55.4
	$1h^2_{9/2}1f_{7/2}0j_{15/2}$	5.1	11.2
	$1h^3_{9/2}0j_{15/2}$	0.9	12.0
	$1f^2_{7/2}0i_{13/2}1g_{9/2}$	9.4	6.5
	$0i^3_{13/2}1g_{9/2}$	8.9	6.3
15^-	$1h^3_{9/2}1g_{9/2}$	83.4	87.0
	$1h^2_{9/2}1f_{7/2}1g_{9/2}$	11.1	9.0

free-nucleon g factors given in table 7.12 of Ref. 34. For orbits not included in this table, we use the average values of the effective operators; in the notation of Arima *et al.*[34] the average correction factors are $\delta_s^{(\pi)} = -2.050$, $\delta_s^{(\nu)} = 1.800$, $\delta_l^{(\pi)} = 0.13$, and $\delta_l^{(\nu)} = -0.08$.

Results are listed in Table XVI where they are compared to experiment. Sjoreen *et al.*[33] listed empirical effective g factors for $\pi 0i_{13/2}$ and $\nu 1g_{9/2}$ of 1.24 and -0.296. The empirical g factor for $\pi 0h_{9/2}$ from ^{209}Bi is 0.913.[20] The predictions calculated with these values substituted for the appropriate Arima values are listed as semiempirical in Table XVI.

The major components of the 11^+ and 15^- wave functions are listed in Table XVII. The rather large difference between the KHP_e and KHP wave functions for the 11^+ state are reflected in the magnetic moments. We note that in either case the wave functions are quite mixed so that calculation of the moment is complicated. It is difficult to say whether the moderate disagreements with experiment evident in Table XVI are due to the wave functions, the effective operators, or a combination of both. However, it is clear that the introduction of configuration mixing via either the KHP_e or KHP interactions improves the agreement significantly.

V. SUMMARY

The KHH and KHP model spaces for nuclei near doubly magic ^{208}Pb are quite different. For the KHH interaction the orbits nearest the Fermi surface have low spin and for the KHP interaction they have high spin. The result is that more orbits are important in the KHH space, but calculations are more difficult in the KHP space. We have found a further difference. Namely, the core-polarization correction of Kuo and Herling appears to be considerably more successful in the KHP space than in the KHH space. By this we mean that energy spectra are best reproduced with values of $K_{\rm ph}$ close to unity for the KHP space while significantly smaller values of $K_{\rm ph}$ are indicated for the KHH space. To understand this one would probably need to look in detail at the specific contributions to the core-polarization corrections in the two model spaces.

For ^{210}Bi we found that the empirical values of $\langle E_J \rangle$ of Eq. (7) for the $\pi 0h_{9/2}\nu 1g_{9/2}$ and $\pi 0h_{9/2}\nu 0j_{15/2}$ configurations were 20% and 17% larger in magnitude than the Kuo-Herling values. This is similar to the findings of 20% and 25% for the empirical to Kuo-Herling ratios for the $(\pi 0h^{-1}_{11/2}\nu 0i^{-1}_{13/2})_{12^-}$ and $(\pi 0h_{9/2}\nu 0i_{11/2})_{10^-}$ TBME of ^{206}Tl and ^{210}Bi reported by Bergstrom *et al.*[16] In Sec. II we touched on the critique of the Kuo-Herling interaction given by Bergstrom *et al.* It is worthwhile to review this critique in more detail as we now do. Bergstrom *et al.* had two points to make.

First, as found in previous studies of the KHH interaction and demonstrated in Sec. III for both the KHH and KHP interactions, the core polarization contribution is generally too repulsive. Bergstrom *et al.* argued convincingly that this is a consequence of the use in the calculation of a constant energy denominator of $\hbar\omega$=14 MeV for the intermediate 1p-1h excitation. Since the particle-hole interaction is generally attractive in isoscaler states and repulsive in isovector states, the collective particle-hole excitations that contribute the bulk of the core-polarization corrections will lie lower (higher) than $2\hbar\omega$ in isoscaler (isovector) modes with the consequence that both modes will give less repulsion. This then offers an explanation for the finding that $K_{\rm ph}$ is generally less than unity.

Their second critique is that the magnitude of $G_{\rm bare}$ is generally too small. This deficiency they attribute to the use of HO radial wave functions in the calculation. An orientation to this deficiency is had by reference to Table XVIII which shows the ratio of overlap integrals calculated with WS and HO wave functions for a few selected TBME. This simple overlap is only proportional to the actual TBME in as far as the effective interaction is dominated by a delta function in the positions of the two nuclei, for instance, if the two-nucleon state is largely ^{3}S. This is the case for the stretched $\pi 0h_j\nu 0i_j$ states considered by Bergstrom *et al.*, but for the $\langle E_J \rangle$ considered here, the comparison only gives a qualitative indication of the difference between the KHP_e and KHP TBME.

TABLE XVIII. Ratios of WS and HO proton-neutron overlap integrals with the orbits i, j, k, m as listed. The HO integral was calculated using $\hbar\omega$ = 7.0 MeV.

Orbits ij	Orbits km	$\frac{\langle i(\pi)j(\nu)\lvert\delta(\mathbf{r}_\pi-\mathbf{r}_\nu)\rvert k(\pi)m(\nu)\rangle_{\rm WS}}{\langle i(\pi)j(\nu)\lvert\delta(\mathbf{r}_\pi-\mathbf{r}_\nu)\rvert k(\pi)m(\nu)\rangle_{\rm HO}}$
$0h_{9/2}0j_{15/2}$	$0h_{9/2}0j_{15/2}$	+1.33
$0i_{13/2}1g_{9/2}$	$0i_{13/2}1g_{9/2}$	+1.04
$0h_{9/2}0j_{15/2}$	$0i_{13/2}1g_{9/2}$	−0.10
$0h_{9/2}1g_{9/2}$	$0h_{9/2}1g_{9/2}$	+1.10
$0h_{9/2}0i_{13/2}$	$0h_{9/2}0i_{13/2}$	+1.29
$0h_{9/2}1g_{9/2}$	$0h_{9/2}0i_{13/2}$	+0.76
$0h_{11/2}0i_{13/2}$	$0h_{11/2}0i_{13/2}$	+1.27

The results of Table XVIII do indeed indicate that the diagonal Kuo-Herling TBME derived from $G_{\rm bare}$ are generally too small in magnitude. They also indicate that the off-diagonal TBME can vary considerably from the values derived with HO wave functions.

In conclusion, we note that a repetition of the Kuo-Herling calculation with realistic radial wave functions for $G_{\rm bare}$ and a more accurate representation of the energy denominator of $G_{\rm 1p1h}$ is feasible. We have demonstrated that the H7B and M3Y potentials can give an accurate account of the Kuo-Herling $G_{\rm bare}$. Thus, one possible approach is to calculate the TBME with these potentials utilizing Woods-Saxon wave functions and then to perform the perturbative calculation of the 1p-1h core-polarization calculation with a more realistic energy denominator than previously used.

ACKNOWLEDGMENTS

We thank G. H. Herling for providing us with the Kuo-Herling matrix elements. Research was supported by the U. S. Department of Energy under Contract No. DE-AC02-76CH00016 with Brookhaven National Laboratory and in part by the National Science Foundation under Grant No. PHY-87-14432 with Michigan State University.

[1] W. W. True and K. W. Ford, Phys. Rev. **109**, 1675 (1958).
[2] T. T. S. Kuo and G. H. Herling, US Naval Research Laboratory Report No. 2258, 1971 (unpublished).
[3] T. T. S. Kuo and G. E. Brown, Nucl. Phys. **85**, 40 (1966).
[4] T. Hamada and I. D. Johnston, Nucl. Phys. **34**, 382 (1962).
[5] J. B. McGrory and T. T. S. Kuo, Nucl. Phys. **A247**, 283 (1975).
[6] J. Blomqvist, L. Rydstrom, R. J. Liotta, and C. Pomar, Nucl. Phys. **A423**, 253 (1984).
[7] B. Harmatz, Nucl. Data Sheets **34**, 735 (1981) (A=210).
[8] M. J. Martin, Nucl. Data Sheets **25**, 397 (1978) (A=211).
[9] M. J. Martin, Nucl. Data Sheets, **27**, 637(1979) (A=212).
[10] A. Hosaka, K.-I. Kubo, and H. Toki, Nucl. Phys. **A244**, 76 (1985).
[11] M. Lacombe, B. Loiseau, J. M. Richard, R. Vinh Mau, J. Côté, P. Pirès, and R. de Tourreil, Phys. Rev. C **21**, 861 (1980).
[12] G. Bertsch, J. Borysowicz, H. McManus, and W. G. Love, Nucl. Phys. **A284**, 399 (1977).
[13] The potential commonly designated M3Y in the literature uses the components labeled 1,4,7,8,11,14,16, and 18 in Table 1 of Ref. 12. The three symbols of the acronyms used in the literature for the H7B and M3Y potentials convey the origin (Hosaka, Michigan), the number of range parameters, and the type of form factor (one-boson-exchange, Yukawa).
[14] R. Reid, Ann. Phys. (N.Y.) **50**, 411 (1968).
[15] Y. K. Gambhir, private communication; F. Monti, G. Bonsignori, M. Savoia, and Y. K. Gambhir, Phys. Rev. C **41**, 1311 (1990).
[16] I. Bergstrom, J. Blomqvist, C. J. Herrlander, and C. G. Lindeén, Research Institute of Physics (Stockholm, Sweden) Annual Report No. 3.3.14 (1976).
[17] B. A. Brown, W. A. Richter, R. E. Julies, and B. H. Wildenthal, Ann. Phys. (N.Y.) **182**, 191 (1988).
[18] B. A. Brown, A. Etchegoyen, W. D. M. Rae, and N. S. Godwin, OXBASH, 1984 (unpublished).
[19] M. R. Schmorak, Nucl. Data Sheets **43**, 383 (1984) (A=207).
[20] M. J. Martin, Nucl. Data Sheets **22**, 545 (1977) (A=209).
[21] S. J. Poletti, G. D. Dracoulis, A. R. Poletti, A. P. Byrne, A. E. Stuchbery, and J. Gerl, Nucl. Phys. **A448**, 189 (1986).
[22] J. Streets, B. A. Brown, and P. E. Hodgson, J. Phys. G **6**, 839 (1983).
[23] P. Mukherjee and B. L. Cohen, Phys. Rev. **127**, 1284 (1962).
[24] J. H. Bjerregaard, O. Hansen, O. Nathan, and S. Hinds, Nucl. Phys. **A94**, 457 (1967),
[25] L. Rydstrom, J. Blomqvist, R. J. Liotta, and C. Pomar, Nucl. Phys. **A512**, 217 (1990).
[26] C. Ellegaard, P. D. Barnes, and E. R. Flynn, Nucl. Phys. **A259**, 435 (1976).
[27] J. P. Schiffer and W. W. True, Rev. Modern Phys. **48**, 191 (1976).
[28] L. G. Mann, K. H. Maier, A. Aprahamian, J. A. Becker, D. J. Decman, E. A. Henry, R. A. Meyer, N. Roy, W. Stöffl, and G. L. Struble, Phys. Rev. C **38**, 74 (1988).
[29] A. E. Stuchbery, G. D. Dracoulis, A. P. Bryne, and A. R. Poletti, Nucl. Phys. **A486**, 397 (1988).
[30] D. Zwarts and P. W. M. Glaudemans, Z. Phys. A **320**, 487 (1985).
[31] R. L. Ponting, R. K. Sheline, E. T. Jurney, L. Nkwambiaya, and B. Bombaka, Rev. Zaïroise Sci. Nucl. **7**, 1 (1986); R. K. Sheline, R. L. Ponting, A. K. Jain, B. bu Nianga, and L. Nkwambiaya, Czech. J. Phys. **B39**, 22 (1989).
[32] J. P. Schiffer, Ann. Phys. (N.Y.) **66**, 798 (1971).
[33] T. P. Sjoreen, U. Garg, D. B. Fossan, J. R. Beene, T. K. Alexander, E. D. Earle, O. Häusser, and A. B. McDonald, Phys. Rev. C **20**, 960 (1979).
[34] A. Arima, K. Shimizu, W. Bentz, and H. Hyuga, *Advances in Nuclear Physics*, edited by J. W. Negele and E. Vogt (Plenum, New York, 1987), Vol. 18, p. 1.